Developmental and Comparative Immunology 41 (2013) 59–67

Contents lists available at SciVerse ScienceDirect

Developmental and Comparative Immunology

journal homepage: www.elsevier.com/locate/dci

Ciona intestinalis peroxinectin is a novel component of the peroxidase–cyclooxygenase gene superfamily upregulated by LPS

Aiti Vizzini, Daniela Parrinello, Maria Antonietta Sanfratello, Valentina Mangano, Nicolò Parrinello, Matteo Cammarata *

Marine Immunobiology Laboratory, Department of Biological Chemical Pharmaceutical Science and Technology, University of Palermo, Via Archirafi 18, Palermo, Italy

ARTICLE INFO

Article history:
Received 11 February 2013
Revised 20 March 2013
Accepted 22 March 2013
Available online 3 April 2013

Keywords:
Ascidian
Peroxinectin
Peroxidase
Inflammation
LPS
Ciona intestinalis

ABSTRACT

Peroxinectins function as hemoperoxidase and cell adhesion factor involved in invertebrate immune reaction. In this study, the ascidian (*Ciona intestinalis*) peroxinectin gene (*Ci*Pxt) and its expression during the inflammatory response have been examined. *Ci*Pxt is a new member of the peroxidase–cyclooxygenase gene superfamily that contains both the peroxidase domain and the integrin KGD (Lys-Gly-Asp) binding motif. A phylogenetic tree showed that *Ci*Pxt is very close to the chordate group and appears to be the outgroup of mammalian MPO, EPO and TPO clades. The *Ci*Pxt molecular structure model resulted superimposable to the human myeloperoxidase. The *Ci*Pxt mRNA expression is upregulated by LPS inoculation suggesting it is involved in *C. intestinalis* inflammatory response. The CiPxt was expressed in hemocytes (compartment/morula cells), vessel epithelium, and unilocular refractile granulocytes populating the inflamed tunic matrix and in the zones 7, 8 and 9 of the endostyle, a special pharynx organs homolog to the vertebrate thyroid gland.

1. Introduction

Enzymes that have peroxidase domains are spread among all the living kingdoms. Phylogenetic analysis clearly reveals that almost all heme peroxidase coding genes have an early origin, and two ubiquitous heme peroxidase superfamilies (peroxidase–cyclooxygenase superfamily and peroxidase–catalase superfamily) represent the main lineages of their development (Zamocky and Obinger, 2010). Although the numerous representatives of the peroxidase–cyclooxygenase superfamily exert a variety of function, the importance of this superfamily is underlined by the numerous enzymes (including human myeloperoxidase, eosinophil peroxidase, and lactoperoxidase) critical in the innate immune responses (Zamocky and Obinger, 2010). Seven main clades representing distinct subfamilies are well segregated in the unrooted phylogenetic tree reconstructed by Zamocky et al. (2008). Even though distinctive mosaic structures can be found, the members of this superfamily share a catalytic domain of about 500 amino acid residues that contains a heme molecule to exert the peroxidase activity.

Peroxinectin, component of the peroxidase–cyclooxygenase superfamily, is characterized by a peroxidase domain and an integrin-binding motif (KGD: Lys-Gly-Asp), and it is mainly spread among various arthropod and nematode species. First, peroxinectin was detected in crayfish hemolymph as a cell adhesion and migration molecule with peroxidase activity (Johansson and Söderhäll, 1988; Johansson et al., 1995; Lin et al., 2007). Cell adhesion and migration are essential mechanisms for development, homeostasis and immunity (Gumbiner, 1996; Ruoslahti and Brink, 1996; Dong et al., 2009). This protein appeared to be involved in hemocyte degranulation (Johansson and Söderhäll, 1989; Cerenius et al., 2008), invasive microorganisms immobilization, phagocytosis, encapsulation, nodule formation (Johansson, 1999; Kobayashi et al., 1990), opsonization (Thornqvist et al., 1994), and transduction pathway regulating the expression of antibacterial peptide genes (Dong et al., 2009). In addition, shrimp peroxinectin activity can be generated by proteolysis related to the activation of the prophenoloxidase system (Sritunyalucksana et al., 2001).

In the phylogenetic tree of peroxidase–cyclooxygenase superfamily, two main invertebrate clades were recognized in peroxinectin subfamily (Zamocky et al., 2008). The first clade includes nematode and squid peroxinectins, whereas the second is formed by insect and crustacean peroxinectins. Among Deuterostomia only a minor subclade of echinozoa (sea urchin *Lytechinus variegates*, *Strongylocentrotus purpuratus* and *Haplochromis pulcherrimus*) peroxinectin sequences have been found, and they resulted very distantly related with any known sequence of vertebrate peroxidases (Zamocky and Obinger, 2010). So far, no sequences from vertebrate peroxinectins are known.

Ascidians occupy a key phylogenetic position and, recently, have been retained the sister group of vertebrates (Swalla et al., 2000; Zeng and Swalla, 2005; Delsuc et al., 2006; Tsagkogeorga

* Corresponding author. Tel.: +39 09123891805.
E-mail address: matteo.cammarata@unipa.it (M. Cammarata).

0145-305X/$ - see front matter © 2013 Elsevier Ltd. All rights reserved.
http://dx.doi.org/10.1016/j.dci.2013.03.015

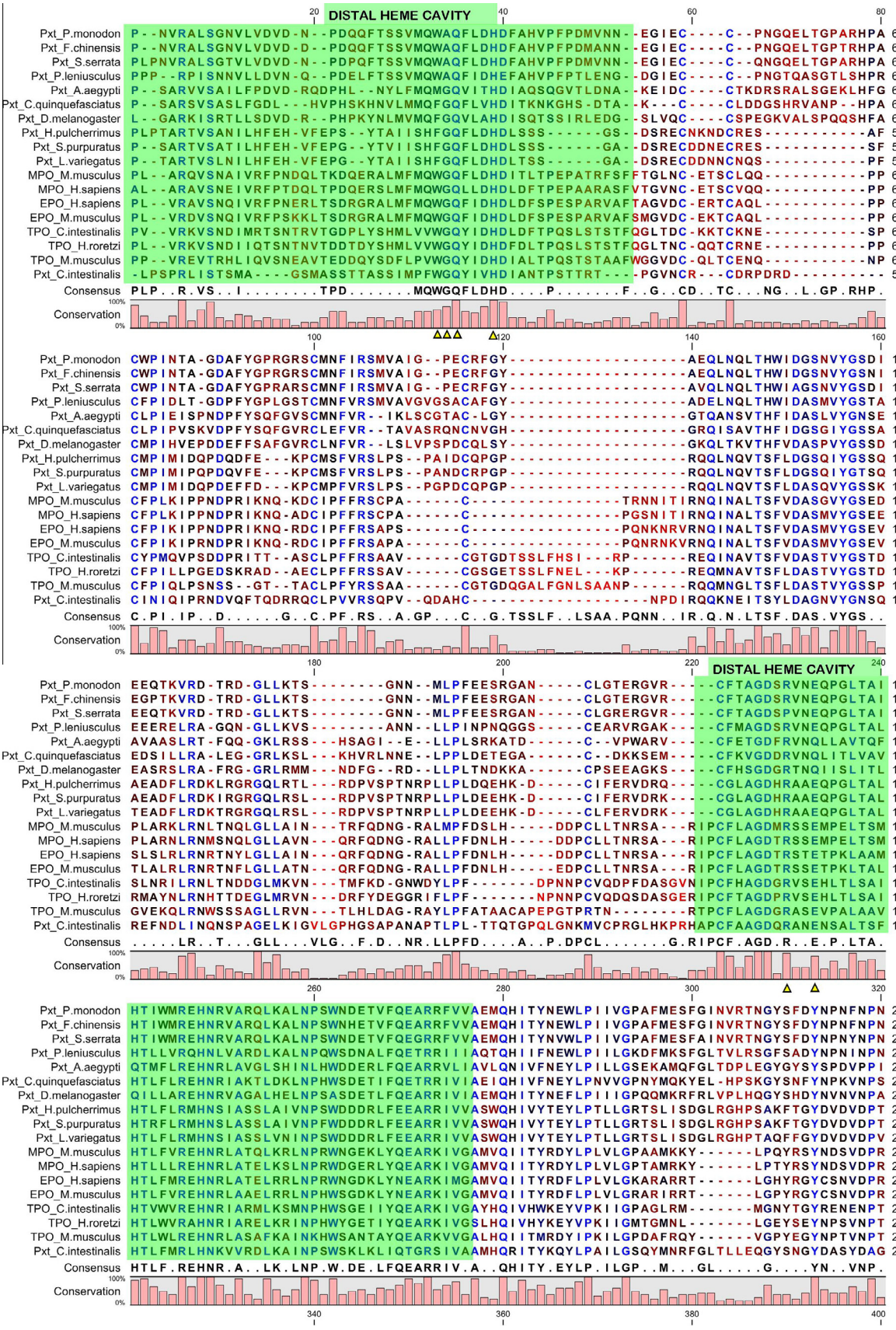

Fig. 1. Alignment of the *Ci*PXT peroxidase domain deduced aminoacid sequence with sequences of peroxidase–cyclooxygenase superfamily components: myeloperoxidase (MPO); eosinophil peroxidase (EPO); thyroid peroxidase (TPO); invertebrate peroxinectins (Pxt). Yellow triangles indicate the conserved amino acids that are known to interact with heme group or calcium. The conservation of amino acid is represented by letter background color gradients (from red to blue). The green boxes indicate the distal (panel A) and proximal (panel B) heme-binding site. (For interpretation of the references to color in this figure legend, the reader is referred to the web version of this article.)

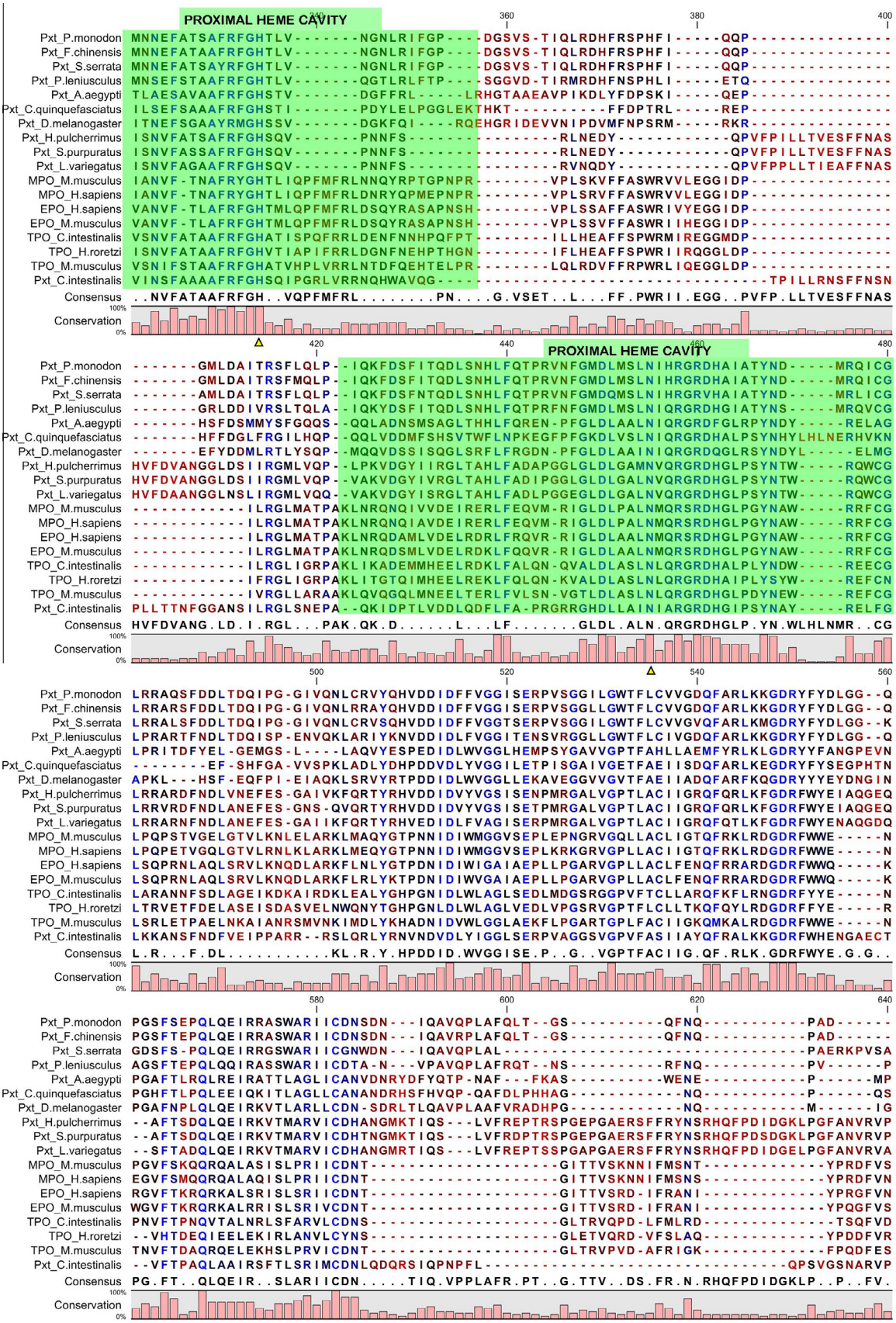

Fig. 1. (*continued*)

et al., 2009). As a result of the knowledge on the genome, *Ciona intestinalis* has become a well-established model to study the evolution of immune components and mechanisms. We first disclosed the *C. intestinalis* inflammatory response (Parrinello, 1981;

Parrinello et al., 1984a,b) and the immune role of the pharynx, where hemocytes (mainly compartment/morula cells) and epithelia express immune related genes (coding type IX collagen-like, TNFα-like, CAP-like and galectin-like proteins) upregulated by lypopolysaccharides (LPS) (Parrinello et al., 2007, 2008, 2010; Vizzini et al., 2008, 2012; Cammarata et al., 2008; Bonura et al., 2009, 2010; Cammarata and Parrinello, 2009). Recently it has also been reported an upregulation of the C3-like gene supporting the immune role of this organ (Giacomelli et al., 2012). The pharynx occupies an extensive part of the adult body, it consists of two epithelial monolayers perforated by dorsoventrally aligned rows of elongated elliptical, ciliated stigmata (Martinucci et al., 1988). Each row of stigmata is enclosed in a mesh of vessels (also called transversal and longitudinal bars), where the hemolymph, containing abundant mature and immature hemocytes, flow. Hemopoietic nodules, associated with the bar epithelia (Ermak, 1976, 1982), can be stimulated by mitogens (Raftos et al., 1991a,b).

In the present paper, we report on *C. intestinalis* peroxinectin (*Ci*Pxt) gene expression (real-time PCR analysis), upregulated by LPS. The CiPxt is a new member of the peroxidase–cyclooxygenase superfamily that contains both the peroxidase domain and the integrin KGD (Lys-Gly-Asp) binding motif. *In situ hybridization* assay revealed that the *Ci*Pxt gene is expressed in hemocytes (compartment/morula cells), epithelium, and unilocular refractile granulocytes populating the inflamed tunic matrix.

2. Material and methods

2.1. Ascidians, LPS inoculation and sample preparation

Ascidians were gathered from Termini Imerese marinas (Italy), maintained in aerated sea water at 15 °C and fed every second day with a marine invertebrate diet (Coraliquid, Sera Heinsberg, Germany). According to previous papers (Vizzini et al., 2008; Cammarata et al., 2008; Parrinello et al., 2008), 100 μg LPS (*Escherichia coli* 055:B5, LPS, Sigma–Aldrich, Germany) in 100 μl of sterile marine solution *per* specimen (MS: 12 mM $CaCl_2$ $6H_2O$, 11 mM KCl, 26 mM $MgCl_2$ $6H_2O$, 43 mM Tris HCl, 0.4 M NaCl, pH 8.0), were inoculated into the median region of the body wall just under the un-vascularized tunic. Ascidians, either untreated (naïve) or injected with 100 μl MS (sham), were used as a control. The ascidian tunic surface was cleaned and sterilized with ethyl alcohol. A suitable amount (200 micrograms/ascidian) of pharynx tissue was excised at various time-points p.i. (1–48 h) from the injection region of the body wall, immediately soaked in RNAlater Tissue collection (Ambion, Austin, TX), and stored at −80 °C.

The hemolymph was withdrawn from the heart with a sterile syringe containing anticoagulant solution (11 mM KCl, 43 mM Tris–HCl, 0.4 M NaCl, 10 mM EDTA, pH 7.4), and centrifuged at 800*g* (10 min, 4 °C), the collected hemocytes were suspended in lysis buffer for RNA isolation with RNAqueous™-Midi Kit purification system (Ambion).

2.2. Total RNA extraction and cDNA synthesis

Total RNA was isolated from the hemocytes and pharynx tissue by using an RNAqueous™-Midi Kit purification system (Ambion) and reverse-transcribed by the Cloned AMV First-Strand cDNA Synthesis Kit (Invitrogen). A PCR reaction was performed using AmpliTaq Gold DNA Polymerase (Applied Biosystems) and *Ci*Pxt 1 forward (GACTTCCCGAAGATAGAATC) and *Ci*Pxt 1 reverse (CCAACAGTACGTGCTCTAAT) primers. The amplification procedure was as follows: 2 min initial denaturation at 95 °C followed by 30 cycles consisting of 95 °C for 30 s; 1 min at the respective annealing temperatures, 72 °C for 1 min and a final extension at 72 °C for 7 min. The amplified fragments were cloned into the pCR™IIvector (TA cloning Kit, Invitrogen) and sequenced. To determine the nucleotide sequence, suitable amounts of lyophilized samples were analyzed by the Biotechnology Centre, University of Padua, Italy. (http://bmr.cribi.unipd.it, ABI PRISM-DNA sequences, Applied Biosystems).

2.3. Phylogenetic and structural analysis

Sequences were subjected to multiple alignments using CLC workbench 6.4. A phylogenetic tree was made by the Neighbor-Joining method (NJ) after 1000 bootstrap iterations by using CLC workbench 6.4.

The accession numbers are as follows: XM_002126249 (*C. intestinalis* peroxinectin), NP_7332264.1 (*Drosophila melanogaster* peroxinectin), EAT44220.1 (*Aedes aegypti* peroxinectin), EDS29893.1 (*Culex quinquefasciatus* peroxinectin), AAL05973.1 (*Penaeus monodon* peroxinectin), ABB55269.2 (*Fenneropenaeus chinensis* peroxinectin), CAA62752.1 (*Pacifastacus leniusculus* peroxinectin), ACF32960. 1 (*Scylla serrata* peroxinectin), CAQ52081.1 (*Mus musculus* myeloperoxidase), AAA59863.1 (*Homo sapiens* myeloperoxidase). EDL36934.1 (*M. musculus* thyroid peroxidase), BAA76688.1 (*C. intestinalis* thyroid peroxidase)BAA76689.1 (*Halocynthia roretzi* thyroid peroxidase), AAA58458.1 (*H. sapiens* eosinophil peroxidase), BAA11370.1 (*M. musculus* eosinophil peroxidase).

The software PEPTIDECUTTER (Gasteiger et al., 2005) was used to search protease cleavage sites. The protein structural models were developed with SWISS-MODEL and the Swiss-PdbViewer (Guex and Peitsch, 1997; Arnold et al., 2006; Schwede et al., 2003) by using human myeloperoxidase isoform C (PBD ID: 1mhlD) as template.

2.4. Real-time PCR analysis

Tissue expression of the *Ci*Pxt gene was examined by real-time PCR analysis with the Sybr-Green method (Applied Biosystems 7500 real-time PCR system), as previously described (Vizzini et al., 2012; Bonura et al., 2010; Parrinello et al., 2008). Primers were designed by using Custom Primers OligoPerfect Designers software (https://tools.invitrogen.com/) and synthesized commercially (Eurofins MWG Operon, Ebersberg, Germany). Tissue expression was performed in a 25-μl PCR containing 2 μl cDNA converted from 250 ng total RNA, 300 nM *Ci*Pxt forward (5′-ACTACACAAACCGGTCCCCAA-3′) and *Ci*Pxt reverse primers (5′-CTGTTTTCGTTTGCCCGTTG-3′), 300 nM actin forward (5′-TGATGTTGCCGCACTCGTA-3′) and actin reverse (5′-TCGACAATGGATCCGGT-3′) primers, and 12.5 μl Power Sybr-Green PCR Master Mix (Applied Biosystems). The 50 cycles of the two-step PCR program consisted of initial polymerase activation for 3 min at 95 °C followed by a denaturing step at 95 °C for 15 s, and then annealing/extension was carried out at 60 °C for 45 s when the fluorescent signal was detected. Each set of samples was run three times, and each plate contained quadruplicate cDNA samples and negative controls. The specificity of amplification was tested by real-time PCR melting analysis. To obtain sample quantification, the $2-\Delta\Delta Ct$ method was used, and the relative changes in gene expression were analyzed as described in the Applied Biosystems Use Bulletin N.2 (P/N 4303859). The amount of *Ci*Pxt transcript from the various tissues was normalized to actin in order to compensate for variations in input RNA amounts. Relative *Ci*Pxt expression was determined by dividing the normalized value of the target gene in each tissue by the normalized value obtained from the untreated tissue.

2.5. Preparation and histology of body wall fragments

The tunic surface was cleaned and sterilized with ethyl alcohol. Body wall fragments (200 mg) containing both tunic and pharynx tissue, were excised from the injection site at various times after

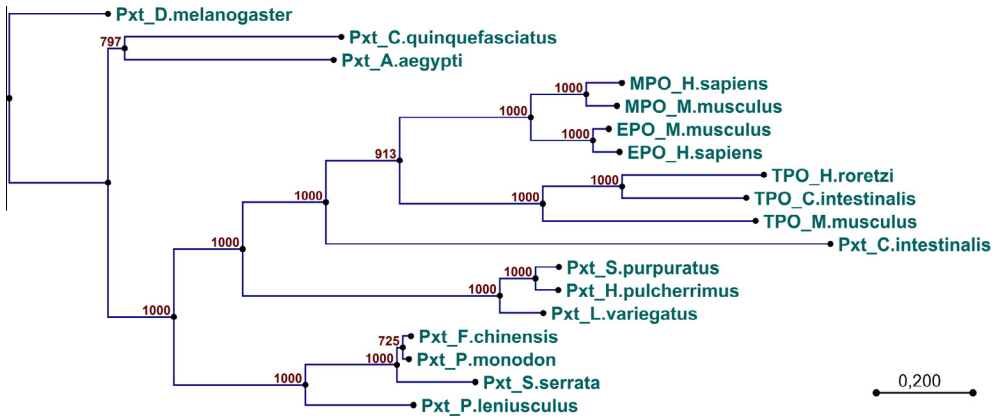

Fig. 2. Phylogenetic tree of peroxidase–cyclooxygenase superfamily: mammalian myeloperoxidase (MPO) and eosinophil peroxidase (EPO); mammalian and ascidian thyroid peroxidase (TPO) and invertebrate peroxinectins (Pxt). The tree was constructed by the neighbor-joining method and bootstrap analysis. Bootstrap value indicates the number particular node occurrences in 1000 trees generated by bootstrapping the sequences. Bar indicate the number of amino acid residues substitutions for site.

the LPS inoculation. For *in situ* hybridization studies, fragments were fixed in Bouin's fluid (saturated picric acid:formaldehyde:acetic acid 15:5:1) for 24 h, paraffin embedded, and serially cut at 6 μm (Leica RM2035 microtome, Solms, Germany).

2.6. In situ hybridization assay (ISH)

To examine gene expression in tissue sections, ISH was carried out with digoxigenin-11-UTP-labeled riboprobes (1 μg/ml final concentration). The *CiPxt* probe was generated by PCR amplifying a cDNA fragment of 519 bp covering the region from nucleotide 2451 to nucleotide 3032 of the isolated cDNA using the *CiPxt* forward oligonucleotide (5′-GACTTCCCGAAGATAGAATC-3′) and the *CiPxt* reverse oligonucleotides (5′-CCAACAGTACGTGCTCTAAT-3′). The digoxigenin-11-UTP-labeled riboprobes was carried out according to manufacturer's instructions (Roche Diagnostics). The re-hydrated histological sections were digested with proteinase K (10 μg/ml) in PBS for 5 min, washed with PBS-T, and treated for hybridization with 50% formamide, 5× SSC (1× SSC: 0.15 M NaCl/0.015 M sodium citrate, pH 7), 50 μg/ml heparin, 500 μg/ml yeast tRNA, and 0.1% Tween 20, at 37 °C overnight. After exhaustive washing in PBS-T and 4XSSC (twice for 10 min), the sections were incubated for 1 h with anti-DIG-Fab-AP conjugate (Roche Diagnostics) diluted 1:500 and washed in PBS-T. Finally, the sections were incubated in the 5-bromo-4-chloro-3-indolyl phosphate/nitro blue tetrazolium liquid substrate system (Sigma–Aldrich, Germany). Color development was stopped after 30 min at room temperature.

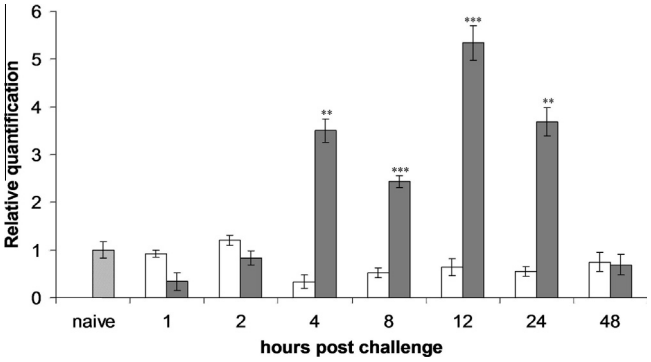

Fig. 4. Real-time PCR analysis. Time-course of *Ci*Pxt gene expression in *Ciona intestinalis* pharynx after inoculation of 100 μg bacterial lipopolysaccharide (LPS) in 100 μl marine solution (MS). To find the significance, the values from LPS-treated ascidians (grey column) were compared with those from ascidians inoculated with 100 μl MS (sham ascidians; white column), while values from sham ascidians were compared with those from naive ascidians. $^{**}P < 0.01$, $^{***}P < 0.001$.

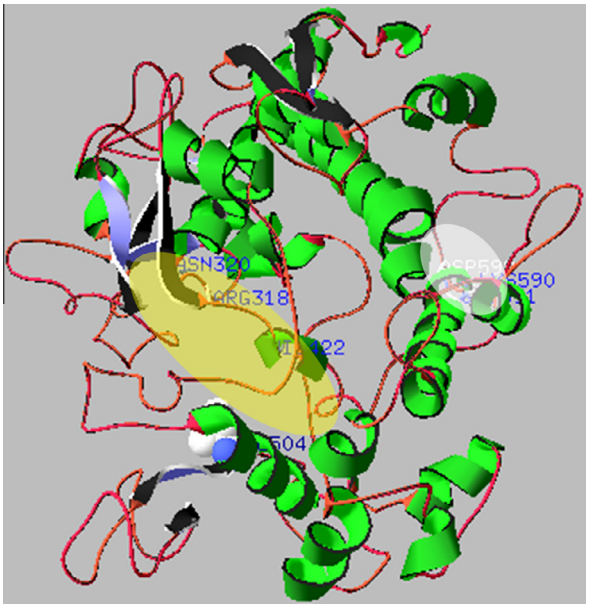

Fig. 3. *Ci*Pxt homology model. The *Ci*Pxt was modeled with the more structural significant overlapping with the crystal structure of human myeloperoxidase isoform C (1mhlD). The heme group position is indicated by an yellow circle; the KGD site is indicated by a white circle. (For interpretation of the references to color in this figure legend, the reader is referred to the web version of this article.)

2.7. Statistical methods

Multiple comparisons were performed with one-way analysis of variance (ANOVA), and different groups were compared by using Tukey's test. Standard deviations were calculated on four experiments. $P < 0.01$ was considered statistically significant.

3. Results

3.1. CiPxt is a new member of the peroxidase–cyclooxygenase superfamily

The entire CiPxt gene sequence was found in a database with an open reading frame (ORF) of 3149 bp (accession number

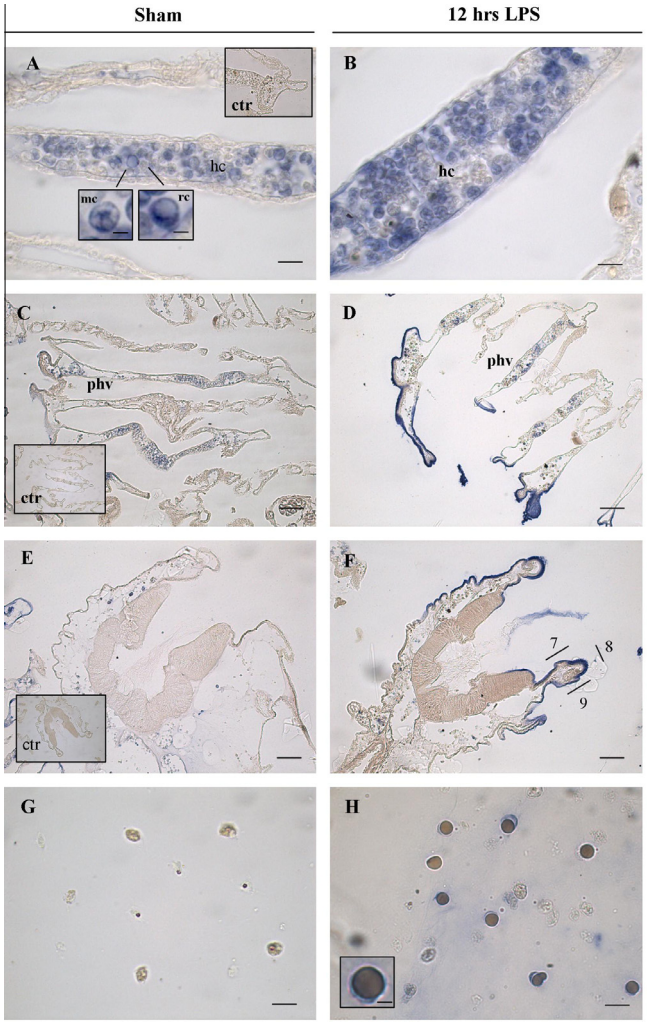

Fig. 5. Histological sections of *Ciona intestinalis* pharynx. *In situ* hybridization with the *Ci*Pxt riboprobe: sham ascidian (A, C, E, G) and ascidian at 12 h after LPS inoculation (B, D, F, H). Vessel (A–D); endostyle (E, F); tunic (G, H). inset: signet ring cells (rc) and compartiment/morula cells (mc) (A), URG (unique retractile granulocyte) (H). Bars size: 40 μm (A, B, G, H); 100 μm (C, D, E, F); 5 μm (insets). phv: pharynx vessels, hc: hemocyte cluster.

XM_002126249 Gene ID: 100177188) encodes a protein of 960 aa with a putative molecular weight of 105 kDa and a predicted isoelectric point of 9.38. Using the program Prosite, a carboxyl-terminal peroxidase domain and an integrin KGD (Lys-Gly-Asp) binding motif were identified. The peroxidase domain is located between 77 and 665 positions. In this domain, the histidine (His^{166}) may be the proton acceptor involved in the peroxidase catalytic fuction, the arginine 318 (Arg^{318}) could be the transition state stabilizer, the histidine (His^{422}) could be a heme binding site, while Cys^{80}-Cys^{94} and Cys^{623}-Cys^{650} indicate intra-chain disuphide linkages. The putative integrin binding motif (Lys-Gly-Asp, KGD) was identified in the C-terminal aminoacid sequence. *Ci*Pxt cDNA was produced by reverse-trascription of mRNA extracted from pharynx and hemocytes of naïve ascidians.

The Signal P-NN program predicted a signal peptide (the first 22 aa) located in the N-terminal region, and provided of the cutting site between Asp^{22} and Ser^{23}.

By using the software PEPTIDECUTTER trypsin cleavage sites were predicted (100% cleavage probability). In particular a total of 70 cleavage sites were found, 2 sites at the N terminal and 25 at the C terminal region. A chymotrypsin cleavage site was also observed.

The *Ci*Pxt deduced amino acid sequence, examined in GeneBank through BLAST analysis (Basic Local Alignment Search Tool), showed significant homologies with peroxidase–cyclooxygenase superfamily members. In particular the highest similarity (S) and identity (I) percentages were found with *Lumbriculus variegatus*, (51% S and 36% I), *S. purpuratus* (51% S and 35% I), *M. musculus* MPO (50% S and 34% I), *M. musculus* TPO (48% S and 33% I).

3.2. Molecular phylogenetic analysis

By using the CLC workbench 6.4. program, the peroxidase domain amino acid sequence of *Ci*Pxt were aligned (Fig. 1) with peroxidase domain sequences of components of peroxidase–cyclooxygenase superfamily including mammalian myeloperoxidase (MPO), eosinophil peroxidase (EPO), thyroid peroxidase (TPO), and invertebrate thyroid peroxidase (TPO) (*C. intestinalis* and *H. roretzi*), peroxinectins (Pxt) from insects (*A. aegypti*, *C. quinquefastacus* and *D. melanogaster*), crustaceans (*S. serrata*, *P. leniusculus*, *P. monodon*, *F. chinensis*) and echinoderm (*L. variegatus, S. purpuratus* and *H. pulcherrimus*). Fig. 1 show amino acid positions conserved in functionally and structurally motif: two on the distal and two on the proximal side of the eme group. Essential distal residue were histidine (His^{166}), the glutamine (Q^{162}), the arginine (R^{318}) and glutamic acid (E^{320}) (Fig. 1A). A conserved motif in mammalian peroxidases is "D-H-D", in *C. intestinalis* this motif is "V-H-D" and includes the distal His^{166} and the Asp^{167}, that have a role as a ligand of calcium. The essential distal glutamine (Q^{162}) is part of a second conserved motif "W/F-G/I/A-Q" present in almost all analyzed sequences (Fig. 1A). The Glutamic acid (E^{320}) is also found in all vertebrate peroxidases, peroxidasins, peroxinectins, peroxicins, and peroxidockerins but is missing in dioxygenases, cyclooxygenases, and dual oxidases. Functionally important motifs on the proximal side peroxidases include the proximal histidine (His^{422}) and its H-bonding partner Asn^{504} (Fig. 1B). Both residues govern the heme iron reactivity by controlling the electron density at the metal.

The phylogenetic tree (Fig. 2) shows an increasing relative distance of the following main clusters: the first one includes chordata MPO, TPO and EPO (i.e. *H. sapiens*, *M. musculus*, *C. intestinalis* and *H. roretzi*), that clearly segregated from the *Ci*Pxt, the second one consists of the echinoid Pxts (i.e. *S. purpuratus*, *H. pulcherrimus*, *L. variegatus*), the third one contains crustacean Pxts, while insect Pxts (i.e. *A. aegypti*, *C. quinquefasciatus*, *D. melanogaster*) form a clearly separated group. Although, the mammalian MPO and EPO (*M. musculus*, *H. sapiens*) are separated from TPO (*M. musculus*, ascidians) branch, they have a significant bootstrap values supporting all branches.

Although *Ci*Pxt is included into the invertebrate Pxts subfamily, it forms, together with the echinozoa *L. variegatus, H. pulcherrimus* and *S. purpuratus*, a deuterostome cluster distinct from the arthropod group that, in turn, is distinguished into crustacean and insect clades.

3.3. Structural analysis

A structural homology analysis was carried out using the SWISS-MODEL program. The homology modeling process was performed on the basis of the known crystal structure of human myeloperoxidase isoform C (1mhlD) (Blair-Johnson et al., 2001). Fig. 3 shows the *Ci*Pxt molecular model resulting from the superimposion of the 181–664 residue sequence that share 34.22% identity (e-value 0.00e−1). The resulting three-dimensional structure shows the KGD (Lys^{580}-Gly^{581}-Asp^{582}) motif localized in a loop in an external position at the end of an α-helix (Fig. 3, white area).

The secondary structure of *Ci*Pxt is predominantly α-helical and each monomer has a central heme-containing core composed of five α-helices (Fig. 3). Both the distal and proximal histidine as well

as its H-bonding partner are located within α-helices (Fig. 3, yellow area).

3.4. CiPxt gene expression is upregulated by LPS

Real time PCR analysis of the inflamed ascidian pharynx showed enhanced *Ci*Pxt mRNA levels as an effect of the LPS challenge (Fig. 4). To examine the time course of the response, four ascidians in three distinct experiments were examined at increasing *post* inoculation time points (1, 2, 4, 8, 12, 24, 48 h). At each time point, four sham ascidians were the controls (fig. 4). The *CiPxt* gene expression significantly boosted at 4 h ($P < 0.01$) and 8 h ($P < 0.001$), reached a maximum value at 12 h ($P < 0.001$) and decreased at 24 h ($P < 0.01$). Then it lowered at 48 h when reached the control levels. The response by sham ascidians indicates that the inoculation procedure did not significantly modulate the mRNA expression.

3.5. In situ hybridization assay (ISH)

Histological sections of the pharynx from ascidians were examined at 12 h following medium (Fig. 5A and C) or LPS inoculation (Fig. 5B and D). Apparently, LPS induces *Ci*Pxt gene upregulation in comparison to the gene expression due to the medium. Fig. 5(A–D) shows that the CiPxt transcript signal is present in tightly packed hemocyte clusters within the vessel lumen and in the vessel epithelium. In Fig. 5(A and B), higher magnifications show *Ci*Pxt-expressing hemocytes, and reveal that compartment/morula cells and signet-ring cells were mainly involved. The riboprobe appears to be localized in a position corresponding to that of the nucleus, at the cell periphery and around the granules of compartment/morula cells. In some pharynx vessels of the LPS-treated ascidians, a larger amount of these cells appeared to be marked by the riboprobe (Fig. 5B). Fig. 5C and D discloses that some regions of the epithelium can also express the transcript. In Fig. 5D, a more intense staining was visible in the histological sections from the LPS treated ascidians. No signal was found in the endostyle of sham ascidians (Fig. 5E), whereas an evident signal was observed in the zones 7, 8 and 9 of this tissue after LPS challenge (Fig. 5F). Finally, the tunic close to the pharynx, was populated with unilocular refractile granulocytes (URGs) many of which contained the probe in the cytoplasm rim around the large granule (Fig. 5H).

4. Discussion

Peroxidases are involved in several important physiological and developmental processes including innate immunity. Peroxidatic heme protein genes appeared very early in evolution, presumably recruited upon pathogen invasion to develop enzyme-dependent unspecific antimicrobial defense closely related with the oxidoreductase substrates. To exert this activity, the enzyme requires the heme group linked in a suitable cavity, and oxidation products are responsible for killing microorganisms (Zederbauer et al., 2007a,b). In mammals, both MPO and EPO are stored in granules of neutrophils, monocytes, and eosinophils, and released at sites of inflammation (Klebanoff, 2005; Wang and Slungaard, 2006). Peroxinectins are provided with a C-terminal peroxidase domain that allows their attribution to the peroxidase–cyclooxygenase superfamily and an N-terminal integrin-binding KGD motif involved in cell adhesion. Interestingly, so far, although no peroxinectins from vertebrate species have been described, many other adhesion proteins have arisen during animal evolution (Parkes and Hart, 2000). Myeloperoxidases have been shown to participate in leukocyte adhesion and trigger cell signaling via alphaMβ2 integrin (Johansson et al., 1997; Lau et al., 2005), and vertebrate myeloperoxidases could be considered both peroxidase and cell-adhesive ligands. Invertebrate peroxinectins, have been shown to be cell-adhesive hemoperoxidases which mediates hemocytes attachment, spreading, degranulation, encapsulation and clearance of invaders (Srituynalucksana et al., 2001; Söderhäll, 1999). The mechanism provides KGD or RGD interplay and integrins receptor of cell surface, as well as cell–extracellular matrix, cell–cell and cell–pathogen interactions (Hynes, 2002).

Biological effects could be due to signal transduction and peroxidase activities. Both the cell adhesion and peroxidase functions can be activated in the presence of LPS or beta-1,3-glucans (Johansson and Söderhäll, 1988; Liu et al., 2005, 2007; Hsu et al., 2006). Peroxinectin also binds Cu–Zn-superoxide dismutase (CuZnSOD) at the surface of circulating hemocytes, and this interaction, facilitated by the close localization, may modulate both the enzyme activities. The hydrogen peroxide, produced by the superoxide dismutases, can be substrate for the peroxinectin. Because PXN has peroxidase activity, this protein might produce hypohalic acid near to the bound pathogen (Cerenius et al., 2008; Johansson, 1999). In invertebrates, peroxinectin genes can be upregulated by LPS or other microbial compounds (Dong et al., 2009; Hsu et al., 2006; Liu et al., 2005), while a peroxinectin-like gene is expressed during oogenesis and early embryogenesis of *D. melanogaster* (Vázquez et al., 2002).

We show that the peroxinectin gene in the *C. intestinalis* pharynx tissues is upregulated by LPS. First, the analysis of the *Ci*Pxt disclosed the phylogenetic relationships of the highly conserved *Ci*Pxt peroxidase domain. The sequence alignment contains four highly conserved regions corresponding to functionally and structurally essential motifs as known from mammalian peroxidases: two on the distal and two on the proximal side of the prosthetic heme group. In particular distal residue histidine is positioned into conserved motif "V-H-D" corresponding to mammalian peroxidase "D-H-D that have a role as a ligand of calcium (Zamocky et al., 2008). The distal glutamine is part of a second conserved motif "W/F-G/I/A-Q" present in almost all the analyzed sequences. Functionally important motifs include the proximal histidine and its H-bonding partner asparagine, likewise the other heme peroxidases superfamily component. The *Ci*Pxt deduced aminoacid sequence aligned well with components (TPO, EPO, MPO) of the peroxidase–cyclooxygenase superfamily, and it appears to be the invertebrate Pxt closest to the mammalian peroxidase group. The phylogentic data could be in accordance to the defense role of mammalian MPO and EPO which are stored in leukocytes and involved in responses to pathogens and inflammation (Wang and Slungaard, 2006). On the contrary, according to Zamocky and Obinger (2010), TPO shows low homology to MPO and EPO that fits with their physiological role in thyroid gland function and supports the notion that the TPO clade branches off very early in the evolution of chordate peroxidases. In this respect, TPO-related enzymes are expressed in the endostyle of the ascidians *C. intestinalis* (Ogosawara et al., 1999), *H. roretzi* (Ogosawara et al., 1999) and of the cephalochordate *Branchiostoma belcheri* (Ogasawara, 2000). The endostyle is a pharyngeal thyroid homolog of vertebrate thyroid glands. Even more, the sequences comparative analysis excluded significant *Ci*Pxt homologies with the mammalian lactoperoxidases released from glands (milk, tears, and saliva) and dual peroxidases that Zamocky and Obinger (2010) reported as a distinct subfamily with totally different enzymatic features (Ihalin et al., 2006). The phylogenetic analysis sorted a TPO chordate clade close to mammalian MPO and EPO, indicating a more recent origin of the ascidian TPOs. The deuterostome echinoid Pxt group lies farthermost from the chordate cluster, and even further distinct is the crustacean Pxt cluster. A functional convergence could be claimed to explain that crustacean peroxinectins are on the major branch together with deuterostomes whereas insect Pxts are clearly

separated. Finally, the remote branch of *D. melanogaster* Pxt could underly its role in development (Vázquez et al., 2002). Finally, a structural homology analysis, resulting from the overlap with the 181–664 residue sequence of human myeloperoxidase (34.22% identity), shows the *Ci*Pxt molecular model. This structure contains the KGD motif as a part of the loop located in an external position at the end of an α-helix. According to previous studies, the Lys-Gly-Asp (KGD) sequence can bind integrins (Hynes, 2002) and participate to cell–cell and cell–extracellular matrix (ECM) interactions.

Finally, *C. intestinalis* Pxt is involved in innate immunity. Several reports suggest that peroxinectin can be essential in cellular defense reaction and resembles the functions of mammalian leukocyte peroxidases (Johansson et al., 1995; Sritunyalucksana et al., 2001; Söderhäll, 1999; Hsu et al., 2006). In crustaceans, they are synthesized and released by semigranular and granular hemocytes in response to foreign stimuli. The exocytosed peroxinectins gain cell adhesion and peroxidase activities by proteolytic processing. Real time PCR analysis recorded an enhanced expression of *C. intestinalis* immune related genes (Parrinello et al., 2008, 2010; Vizzini et al., 2008, 2012; Cammarata et al., 2008; Bonura et al., 2009, 2010; Cammarata and Parrinello, 2009) in the pharynx tissues which generate water current and come in contact with a large variety of microbes exerting an early recognition of PAMPs. Therefore we primarily examined this organ, and disclosed that the *Ci*Pxt gene expression can be enhanced by LPS inoculation suggesting the *Ci*Pxt involvement in the inflammatory response. The real time PCR profile shows that, after a first increase at 4 h p.i. and a decrease at 8 h, an significant expression was found at 12 and 24 h p.i. Since previous findings indicated that inflammatory gene expression could be more prompt (4–8 h), the possibility exists that the *Ci*Pxt 24 h late response could be dependent on LPS persistence in this tissues and/or on the complex inflammatory mechanism that involves the expression of several inflammatory molecules (Parrinello et al., 2007, 2008, 2010; Vizzini et al., 2008, 2012; Cammarata et al., 2008; Bonura et al., 2009, 2010; Cammarata and Parrinello, 2009). Hemocytes (compartment/morula cells, signet-ring cells and URGs), already known to be involved in the pharynx inflammatory response, express the *Ci*Pxt gene. Although, precise quantitative data were not derived from the histological observations, according to previous papers (Parrinello et al., 2008, 2010; Vizzini et al., 2008, 2012; Cammarata et al., 2008; Bonura et al., 2009, 2010; Cammarata and Parrinello, 2009), an increased number of *Ci*Pxt-positive compartment/morula cells and signet-ring cells in the vessels as well as positive regions of the vessel epithelium, can be related to LPS inoculation that upregulates immune-related genes. Furthermore, an evident involvement of a large number of *Ci*Pxt expressing URGs in the inflamed tunic matrix was also disclosed. This tissue was intensely populated with URGs, usually poor in the controls. URGs are specific hemocytes that contain a unique granule that occupies most the cytoplasm, furthermore express phenoloxidase (Parrinello et al., 2003). In this contest, it is known that LPS activates the prophenoloxidase (proPO) system through proteolytic cleavage (Cammarata et al., 2008). A cascade of proteinases cleaves proPO into active PO and similarly to other invertebrate could activates properoxinectin into peroxinectin (Cerenius et al., 2008). It is noteworthy that LPS stimulates the *Ci*Pxt gene expression by the endostyle cells.

The endostyle is a ventral midline organ of the pharynx in early cordates, and it is retained an evolutionary precursor of the vertebrate tyroid gland. The morphogenesis of this gland, that originates from the embryonic pharyngeal epithelium, supports the homology. In addition, endostyle incorporates iodine (Barrington, 1957, 1958; Salvatore, 1969), and the expression of homolog thyroid-specific developmental genes during endostyle development has been reported (McCauley and Bronner-Fraser, 2002; Ogasawara, 2000; Ogasawara and Satoh, 1998; Ogasawara et al., 2001; Venkatesh et al., 1999). The zones 7, 8 and 9 of the *C. intestinalis* endostyle have been retained the endostyle regions homologs to the vertebrate thyroid (Ogasawara and Satoh, 1998), disclose peroxidase activity (Fujita and Sawano, 1979; Kobayashi et al., 1983), and a specific TPO has been identified in the zone 7 (Ogosawara et al., 1999). Although a relation between *Ci*Pxt and peroxidase activity could be hypothesized, the present data on *Ci*Pxt expression by these zones do not allow to establish a relationship between *Ci*Pxt gene expression and thyroid-like activity during the inflammatory response. However, it is known that, in humans, pro-inflammatory cytokines cause thyroid inflammatory disorders (Ajjan et al., 1996) and a recent paper reports on thyroid cells that express functional sensors for exogenous and endogenous dangers, and they are capable of launching innate immune responses without the assistance of immune cells (Kawashima et al., 2012).

In conclusion, our results provide compelling evidence of a complex involvement of the pharynx in *C. intestinalis* innate immunity.

Acknowledgements

This work was supported by a research grant from the Italian Ministry of Education (PRIN 2006 and 2010-2011 to N. Parrinello), co-funded by the University of Palermo. We thank M. Guarcello for collecting ascidians for maintenance of the aquaria.

References

Ajjan, R.A., Watson, P.F., Weetman, A.P., 1996. Cytokines and thyroid function. Adv. Neuroimmunol. 6, 359–386.
Arnold, M.S., Green, A.A., Hulvat, J.F., Stupp, S.I., Hersam, M.C., 2006. Sorting carbon nanotubes by electronic structure using density differentiation. Nat. Nanotechnol. 1, 60–65.
Barrington, E.J.W., 1957. The distribution and significance of organically bound iodine in the ascidian *Ciona intestinalis* Linnaeus. J. Mar. Biol. Assoc. U.K. 36, 1–16.
Barrington, E.J.W., 1958. The localization of organically bound iodine in the endostyle of Amphioxus. J. Mar. Biol. Assoc. U.K. 37, 117–126.
Blair-Johnson, M., Fiedler, T., Fenna, R., 2001. Human myeloperoxidase: structure of a cyanide complex and its interaction with bromide and thiocyanate substrates at 1.9 Å resolution. Biochemistry 40 (46), 13990–13997.
Bonura, A., Vizzini, A., Salerno, G., Parrinello, N., Longo, V., Colombo, P., 2009. Isolation and expression of a novel MBL-like collectin cDNA enhanced by LPS injection in the body wall of the ascidian *Ciona intestinalis*. Mol. Immunol. 46, 2389–2394.
Bonura, A., Vizzini, A., Salerno, G., Parrinello, D., Parrinello, N., Longo, V., Montana, G., Colombo, P., 2010. Cloning and expression of a novel component of the CAP superfamily enhanced in the inflammatory response to LPS of the ascidian *Ciona intestinalis*. Cell Tissue Res. 342, 411–421.
Cammarata, M., Arizza, V., Cianciolo, C., Parrinello, D., Vazzana, M., Vizzini, A., Salerno, G., Parrinello, N., 2008. The prophenoloxidase system is activated during the tunic inflammatory reaction of *Ciona intestinalis*. Cell Tissue Res. 333, 481–492.
Cammarata, M., Parrinello, N., 2009. The ascidian prophenoloxidase activating system. Invert. Surviv. J 6, 67–76.
Cerenius, L., Lee, B.L., Söderhäll, K., 2008. The proPO-system: pros and cons for its role in invertebrate immunity. Trends Immunol. 29, 263–271.
Delsuc, F., Brinkmann, H., Chourrout, D., Philippe, H., 2006. Tunicates and not cephalochordates are the closest living relatives of vertebrates. Nature 439, 965–968.
Dong, B., Liu, F., Gao, H., Wang, B., Xiang, J., 2009. CDNA cloning and gene expression pattern following bacterial challenge of peroxinectin in Chinese shrimp *Fenneropenaeus chinensis*. Mol. Biol. Rep. 36, 2333–2339.
Ermak, T.H., 1976. The hematogenic tissues of Tunicates. In: Wright, R.K., Cooper, E.L. (Eds.), Phylogeny of Thymus and Bone Marrow-Bursa Cells. Elsevier, Amsterdam, North Holland, pp. 45–56.
Ermak, T.H., 1982. The renewing cell populations of ascidians. Am. Zool. 22, 795–805.
Fujita, H., Sawano, F., 1979. Fine structural localization of endogeneous peroxidase in the endostyle of ascidians, *Ciona intestinalis*. A part of phylogenetic studies of the thyroid gland. Arch. Histol. Jpn. 42, 319–326.
Gasteiger, E., Hoogland, C., Gattiker, A., Duvaud, S., Wilkins, M.R., Appel, R.D., Bairoch, A., 2005. Protein identification and analysis tools on the ExPASy server. In: Walker, J.M. (Ed.), The Proteomics Protocols Handbook. Humana Press, Totowa, USA, pp. 571–607.

Giacomelli, S., Melillo, D., Lambris, J.D., Pinto, M.R., 2012. Immune competence of the *Ciona intestinalis* pharynx: complement system-mediated activity. Fish Shellfish Immunol. 33, 946–952.
Guex, N., Peitsch, M.C., 1997. SWISS-MODEL and the Swiss-PdbViewer: an environment for comparative protein modelling. Electrophoresis 18, 2714–2723.
Gumbiner, B.M., 1996. Cell adhesion: the molecular basis of tissue architecture and morphogenesis. Cell 84, 345–357.
Hsu, P.I., Liu, C.H., Tseng, D.Y., Lee, P.P., Cheng, W., 2006. Molecular cloning and characterisation of peroxinectin, a cell adhesion molecule, from the giant freshwater prawn *Macrobrachium rosenbergii*. Fish Shellfish Immunol. 21, 1–10.
Hynes, R.O., 2002. Integrins: bidirectional, allosteric signaling machines. Cell 110, 673–687.
Ihalin, R., Loimaranta, V., Tenovuo, J., 2006. Origin, structure, and biological activities of peroxidases in human saliva. Arch. Biochem. Biophys. 445, 261–268.
Johansson, M.W., Patarroyo, M., Oberg, F., Siegbahn, A., Nilsson, K., 1997. Myeloperoxidase mediates cell adhesion via the alpha M beta 2 integrin (Mac-1, CD11b/CD18). J. Cell Sci. 110 (9), 1133–1139.
Johansson, M.W., 1999. Cell adhesion molecules in invertebrate immunity. Dev. Comp. Immunol. 23, 303–315.
Johansson, M.W., Lind, M.I., Holmblad, T., Thörnqvist, P.O., Söderhäll, K., 1995. Peroxinectin, a novel cell adhesion protein from crayfish blood. Biochem. Biophys. Res. Commun. 216, 1079–1087.
Johansson, M.W., Söderhäll, K., 1988. Isolation and purification of a cell adhesion factor from crayfish blood cells. J. Cell Biol. 106, 1795–1803.
Johansson, M.W., Söderhäll, K., 1989. A cell adhesion factor from crayfish haemocytes has degranulating activity towards crayfish granular cells. Insect Biochem. 19, 183–190.
Kawashima, A., Yamazaki, K., Hara, T., Akama, T., Yoshihara, A., Sue, M., Tanigawa, K., Wu, H., Ishido, Y., Takeshita, F., Ishii, N., Sato, K., Suzuki, K., 2012. Thyroid. http://dx.doi.org/10.1089/thy.2011.0480.
Klebanoff, J.S., 2005. Myeloperoxidase: friend and foe. J. Leukoc. Biol. 77, 598–625.
Kobayashi, H., Tsuneki, K., Akiyoshi, H., Kobayashi, Y., Nozaki, M., Ouji, M., 1983. Histochemical distributionof peroxidase in ascidians with special reference to the endostyle and the branchial sac. Gen. Comp. Endocrinol. 50, 172–187.
Kobayashi, M., Johansson, M.W., Söderhäll, K., 1990. The 76 kDa cell adhesion factor from crayfish haemocytes promotes encapsulation *in vitro*. Cell Tissue Res. 260, 113–118.
Lau, D., Mollnau, H., Eiserich, J.P., Freeman, B.A., Daiber, A., Gehling, U.M., Brümmer, J., Rudolph, V., Münzel, T., Heitzer, T., Meinertz, T., Baldus, S., 2005. Myeloperoxidase mediates neutrophil activation by association with CD11b/CD18 integrins. PNAS 102, 431–436.
Lin, X., Cerenius, L., Lee, B.L., Söderhäll, K., 2007. Purification of properoxinectin myeloperoxidase homologue and its activation to a cell adhesion molecule. Biochem. Biophys. Acta 170, 87–93.
Liu, C.H., Cheng, W., Chen, J.C., 2005. The peroxinectin of white shrimp *Litopenaeus vannamei* is synthesised in the semi-granular and granular cells, and its transcription is up-regulated with *Vibrio alginolyticus* infection. Fish Shellfish Immunol. 18, 431–444.
Liu, C.H., Yeh, S.P., Hsu, P.Y., Cheng, W., 2007. Peroxinectin gene transcription of the giant freshwater prawn *Macrobrachium rosenbergii* under intrinsic, immunostimulant, and chemotherapeutant influences. Fish Shellfish Immunol. 22, 408–417.
Martinucci, G.B., Dallai, R., Burighel, P., Lane, N.J., 1988. Different functions of tightjunctions in the ascidian branchial basket. Tissue Cell 20, 119–132.
McCauley, D.W., Bronner-Fraser, M., 2002. Conservation of Pax gene expression in ectodermal placodes of the lamprey. Gene 287, 129–139.
Ogasawara, M., Satoh, N., 1998. Isolation and characterization of endostyle-specific genes in the ascidian *Ciona intestinalis*. Biol. Bull. 195, 60–69.
Ogosawara, M., Di Lauro, R., Satoh, N., 1999. Ascidian homologs of mammalian thyroid peroxidase genes are expressed in the thyroid-equivalent region of the endostyle. J. Exp. Zool. 285, 158–169.
Ogasawara, M., 2000. Overlapping expression of amphioxus homologs of the thyroid transcription factor-1 gene and thyroid peroxidase gene in the endostyle: insight into evolution of the thyroid gland. Dev. Genes Evol. 210, 231–242.
Ogasawara, M., Shigetani, Y., Suzuki, S., Kuratani, S., Satoh, N., 2001. Expression of thyroid transcription factor-1 (TTF-1) gene in the ventral forebrain and endostyle of the agnathan vertebrate, *Lampetra japonica*. Genesis 30, 51–58.
Parkes, R.J., Hart, S.L., 2000. Adhesion molecules and gene transfer. Adv. Drug Deliv. Rev. 44, 135–152.
Parrinello, N., 1981. The reaction of *Ciona intestinalis* L. To subcuticular erythrocyte and protein injection. Dev. Comp. Immunol. 5, 105–110.
Parrinello, N., Patricolo, E., Canicattì, C., 1984a. Inflammatory-like reaction in the tunic of *Ciona intestinalis* (Tunicata). Encapsulation and tissue injury I. Biol. Bull. 167, 229–237.
Parrinello, N., Patricolo, E., Canicattì, C., 1984b. Inflammatory-like reaction in the tunic of *Ciona intestinalis* (Tunicata). Encapsulation tissue injury II. Biol. Bull. 167, 238–250.
Parrinello, N., Arizza, V., Chinnici, C., Parrinello, D., Cammarata, M., 2003. Phenoloxidases in ascidian hemocytes: characterization of the pro-phenoloxidase activating system. Comp. Biochem. Physiol. 135B, 583–591.
Parrinello, N., Arizza, V., Cammarata, M., Giaramita, F.T., Pergolizzi, M., Vazzana, M., Vizzini, A., Parrinello, D., 2007. Inducible lectins with galectin properties and human IL1alpha epitopes opsonize yeast during the inflammatory response of the ascidian *Ciona intestinalis*. Cell Tissue Res. 329, 379–390.
Parrinello, N., Vizzini, A., Arizza, V., Salerno, G., Parrinello, D., Cammarata, M., Giaramita, F.T., Vazzana, M., 2008. Enhanced expression of a cloned and sequenced *Ciona intestinalis* TNF alpha-like (CiTNF alpha) gene during the LPS-induced inflammatory response. Cell Tissue Res. 334, 305–317.
Parrinello, N., Vizzini, A., Salerno, G., Sanfratello, M.A., Cammarata, M., Arizza, V., Vazzana, M., Parrinello, D., 2010. Inflamed adult pharynx tissues and swimming larva of *Ciona intestinalis* share CiTNF alpha-producing cells. Cell Tissue Res. 341, 299–311.
Raftos, D.A., Cooper, E.L., Habicht, G.S., Beck, G., 1991a. Invertebrate cytokines: tunicate cell proliferation stimulated by an interleukin 1-like molecule. Proc. Natl. Acad. Sci. U.S.A. 88, 9518–9522.
Raftos, D.A., Stillman, D.L., Cooper, E.L., 1991b. Interleukin-2 and phytohaemagglutinin stimulate the proliferation of tunicate cells. Immunol. Cell Biol. 69, 225–234.
Ruoslahti, E., Brink, B., 1996. Common principles in cell adhesion. Exp. Cell Res. 227, 1–11.
Salvatore, G., 1969. Thyroid hormone biosynthesis in Agnatha and Protochordata. Gen. Comp. Endocrinol. (Suppl. 2), 535–550.
Schwede, T., Kopp, J., Guex, N., Peitsch, M.C., 2003. SWISS-MODEL: an automated protein homology-modeling server. Nucleic Acids Res. 31, 3381–3385.
Söderhäll, K., 1999. Invertebrate immunity. Dev. Comp. Immunol. 23, 263–266.
Sritunyalucksana, K., Wongsuebsantati, K., Johansson, M.W., Söderhäll, K., 2001. A cell adhesive protein associated with the proPO system from the black tiger shrimp, *Penaeus monodon*. Dev. Comp. Immunol. 25, 353–363.
Swalla, B.J., Cameron, C.B., Corley, L.S., Garey, J.R., 2000. Urochordates are monophyletic within the deuterostomes. Rev. Syst. Biol. 49, 52–64.
Thornqvist, P.O., Johansson, M.W., Söderhäll, K., 1994. Opsonic activity of cell adhesion protein and b-1, 3-glucan-binding proteins from two crustaceans. Dev. Comp. Immunol. 18, 3–12.
Tsagkogeorga, G., Turon, X., Hopcroft, R.R., Tilak, M.K., Feldstein, T., Shenkar, N., Loya, Y., Huchon, D., Douzery, E.J., Delsuc, F., 2009. An updated 18S rRNA phylogeny of tunicates based on mixture and secondary structure models. BMC Evol. Biol. 5, 9–187.
Vázquez, M., Rodríguez, R., Zurita, M., 2002. A new peroxinectin-like gene preferentially expressed during oogenesis and early embryogenesis in *Drosophila melanogaster*. Dev. Genes Evol. 212, 526–529.
Venkatesh, T.V., Holland, N.D., Holland, L.Z., Su, M.T., Bodmer, R., 1999. Sequence and developmental expression of AmphiNk2-1: insights into the evolution of the vertebrate thyroid gland and forebrain. Dev. Genes Evol. 209, 254–259.
Vizzini, A., Pergolizzi, M., Vazzana, M., Salerno, G., Di Sano, C., Macaluso, P., Arizza, V., Parrinello, D., Cammarata, M., Parrinello, N., 2008. FACIT collagen (1alpha-chain) is expressed by hemocytes and epidermis during the inflammatory response of the ascidian *Ciona intestinalis*. Dev. Comp. Immunol. 32, 682–692.
Vizzini, A., Parrinello, D., Sanfratello, M.A., Salerno, G., Cammarata, M., Parrinello, N., 2012. Inducible galectins are expressed in the inflamed pharynx of the ascidian *Ciona intestinalis*. Fish Shellfish Immunol. 32, 101–109.
Wang, J., Slungaard, A., 2006. Role of eosinophil peroxidase in host defense and disease pathology. Arch. Biochem. Biophys. 15, 256–260.
Zamocky, M., Jakopitsch, C., Furtmuller, P.G., Dunand, C., Obinger, C., 2008. The peroxidase–cyclooxygenase superfamily: reconstructed evolution of critical enzymes of the innate immune system. Proteins 72, 589–605.
Zamocky, M., Obinger, C., 2010. Molecular phylogeny of heme peroxidases. In: Torres, E., Ayala, M. (Eds.), Biocatalysis Based on Heme Peroxidases. Springer-Verlag, Berlin Heidelberg, pp. 7–35.
Zederbauer, M., Furtmuller, P.G., Bellei, M., Stampler, J., Jakopitsch, C., Battistuzzi, G., Moguilevsky, N., Obinger, C., 2007a. Disruption of the aspartate to heme ester linkage in human myeloperoxidase: impact on ligand binding, redox chemistry and interconversion of redox intermediates. J. Biol. Chem. 282, 17041–17052.
Zederbauer, M., Furtmuller, P.G., Ganster, B., Moguilevsky, N., Obinger, C., 2007b. Manipulating the vinyl-sulfonium bond in human myeloperoxidase: impact on compound I formation and reduction by halides and thiocyanate. Biochem. Biophys. Res. Commun. 356, 450–456.
Zeng, L., Swalla, B.J., 2005. Molecular phylogeny of the protochordates: chordate evolution. Can. J. Zool. 83, 24–33.